Electron Paramagnetic Resonance and Electron−Nuclear Double Resonance Studies of the Reactions of Cryogenerated Hydroperoxoferric−Hemoprotein Intermediates

ARTICLE *in* BIOCHEMISTRY · JULY 2014

Impact Factor: 3.02 · DOI: 10.1021/bi500296d · Source: PubMed

6 AUTHORS, INCLUDING:

Roman Davydov

Northwestern University

134 PUBLICATIONS **2,534** CITATIONS

SEE PROFILE

Amy Ledbetter-Rogers

College of Charleston

2 PUBLICATIONS **90** CITATIONS

SEE PROFILE

BIOCHEMISTRY
including biophysical chemistry & molecular biology

Article

pubs.acs.org/biochemistry

Electron Paramagnetic Resonance and Electron-Nuclear Double Resonance Studies of the Reactions of Cryogenerated Hydroperoxoferric−Hemoprotein Intermediates

Roman Davydov,[†] Mikhail Laryukhin,[†] Amy Ledbetter-Rogers,[‡] Masanori Sono,[§] John H. Dawson,*[,§] and Brian M. Hoffman*[,†]

[†]Department of Chemistry, Northwestern University, 2145 Sheridan Road, Evanston, Illinois 60208-3113, United States
[‡]Department of Chemistry and Biochemistry, College of Charleston, Charleston, South Carolina 29424, United States
[§]Department of Chemistry and Biochemistry, University of South Carolina, Columbia, South Carolina 29208, United States

Supporting Information

ABSTRACT: The fleeting ferric peroxo and hydroperoxo intermediates of dioxygen activation by hemoproteins can be readily trapped and characterized during cryoradiolytic reduction of ferrous hemoprotein−O_2 complexes at 77 K. Previous cryoannealing studies suggested that the relaxation of cryogenerated hydroperoxoferric intermediates of myoglobin (Mb), hemoglobin, and horseradish peroxidase (HRP), either trapped directly at 77 K or generated by cryoannealing of a trapped peroxo-ferric state, proceeds through dissociation of bound H_2O_2 and formation of the ferric heme without formation of the ferryl porphyrin π-cation radical intermediate, compound I (Cpd I). Herein we have reinvestigated the mechanism of decays of the cryogenerated hydroperoxyferric intermediates of α- and β-chains of human hemoglobin, HRP, and chloroperoxidase (CPO). The latter two proteins are well-known to form spectroscopically detectable quasistable Cpds I. Peroxoferric intermediates are trapped during 77 K cryoreduction of oxy Mb, α-chains, and β-chains of human hemoglobin and CPO. They convert into hydroperoxoferric intermediates during annealing at temperatures above 160 K. The hydroperoxoferric intermediate of HRP is trapped directly at 77 K. All studied hydroperoxoferric intermediates decay with measurable rates at temperatures above 170 K with appreciable solvent kinetic isotope effects. The hydroperoxoferric intermediate of β-chains converts to the S = 3/2 Cpd I, which in turn decays to an electron paramagnetic resonance (EPR)-silent product at temperature above 220 K. For all the other hemoproteins studied, cryoannealing of the hydroperoxo intermediate directly yields an EPR-silent majority product. In each case, a second follow-up 77 K γ-irradiation of the annealed samples yields low-spin EPR signals characteristic of cryoreduced ferrylheme (compound II, Cpd II). This indicates that in general the hydroperoxoferric intermediates relax to Cpd I during cryoanealing at low temperatures, but when this state is not captured by reaction with a bound substrate, it is reduced to Cpd II by redox-active products of radiolysis.

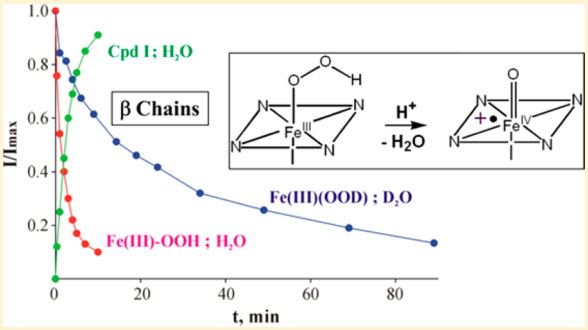

Radiolytic cryoreduction and cryooxidation in combination with various spectroscopic techniques have found widespread application in the study of metalloprotein intermediates and the mechanisms of their reactions.[1] In particular, application of this approach has led to important advances in our understanding of the catalytic mechanisms of heme monooxygenases[1−4] such as cytochromes P450,[2,5−10] which catalyze the reductive activation of dioxygen and are involved in biological processes such as the biosynthesis of biologically active compounds such as steroids and detoxification of xenobiotics,[11−14] of nitric oxide synthase (NOS),[4,15] which generates NO as a signaling molecule,[16,17] and of heme oxygenases,[3,18] whose role in the oxidative breakdown of heme itself is of great medical interest.[13,19,20] The combination electron paramagnetic resonance (EPR) and electron-nuclear double resonance (ENDOR) spectroscopies with 77 K cryoreduction techniques has shown that the primary cryotrapped products of one-electron reduction of oxyferrous cytochrome P450cam, heme oxygenase, and oxyferrous NOS are peroxoferric or hydroperoxoferric heme intermediates or both (Fe(III)−O_2^{2-}/Fe(III)−OOH^-), Scheme 1, which exhibit characteristic EPR and ENDOR spectra.[1] These products of 77 K cryoreduction are trapped in the conformation(s) of the parent oxy-ferrous state and provide sensitive EPR/ENDOR probes for studying structural features of the parent state.

In the case of heme oxygenase, the hydroperoxo intermediate was shown to carry out the first step of heme biodegradation, namely, conversion of the heme into α-meso-hydroxy-

Received: March 10, 2014
Revised: July 8, 2014
Published: July 21, 2014

   dx.doi.org/10.1021/bi500296d | Biochemistry 2014, 53, 4894−4903

Scheme 1

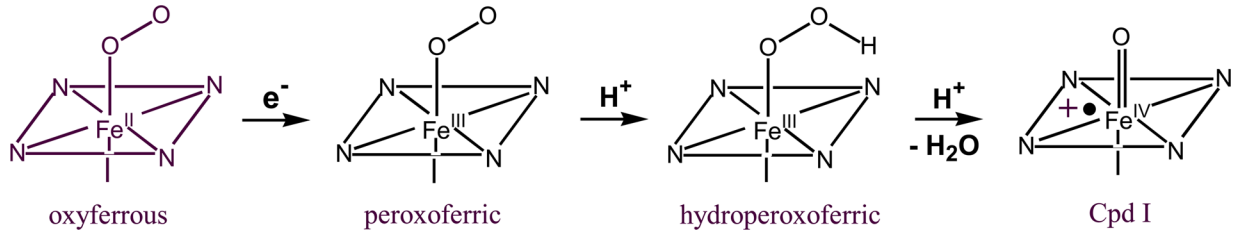

heme.[3,8,19] Peroxo/hydroperoxo intermediates were shown to participate in the conversion of *N*-hydroxyarginine (NOHA) into NO and citrulline catalyzed by nitric oxide synthase (NOS).[4] In contrast, compound I (Cpd I), arising from proton-assisted heterolytic cleavage of the O−O bond of the ligand in hydroperoxoferric intermediates, is the catalytically active oxygenating species in the monooxygenase cycles catalyzed by cytochromes P450 and in argininine hydroxylation by NOS.[1,4]

Despite the central role of Cpd I in the enzymatic mechanism of cytochromes P450, NOS, and peroxidases, Cpd I is not spectroscopically detected during the relaxation of the cryogenerated hydroperoxo-ferriheme state in frozen solutions of the oxy complexes of a majority of hemoproteins, including cytochromes P450, NOS, horseradish peroxidase (HRP), and *Caldariomyces fumago* chloroperoxidase (CPO).[1,2,4,6,15,21,22] This is surprising because Cpds I of HRP and CPO are relatively stable in fluid solution at subzero temperatures;[23,24] a P450 Cpd I has been trapped and characterized.[25−27] In addition, Cpds I were observed recently during decay of cryogenerated substrate-free hydroperoxoferric dehaloperoxidase (DHP)[28] and in crystals of oxy-Hrp radiolytically reduced at 77 K.[29]

Three possible explanations have been proposed for the failure to observe Cpd I during cryoreduction/annealing of oxy-hemoproteins: (i) Cpd I does not form during relaxation of the hydroperoxoferric state because, as suggested by Denisov et al.[22] and Symons and co-workers,[30] the cryogenerated hydroperoxyferriheme intermediates decay via dissociation of H_2O_2 at low temperatures; (ii) the highly reactive ferryl centers in Cpd I are reduced at low temperatures by redox-active radical products of the cryoradiolysis; and (iii) as in reactions with organic peroxides, the oxo-Fe(IV) porphyrin π-cation radical centers in NOS and cytochrome P450cam Cpds I oxidize nearby amino acid residues at high rates[1,31] to form EPR-silent (S = 1) oxo-Fe(IV)porphyrin

Herein, we report cryoannealing investigations of the mechanism of decay of hydroperoxoferric hemoproteins formed through 77 K radiolytic cryoreduction, which uses EPR/ENDOR spectroscopy at liquid He temperatures as the probe, as applied to a suite of oxy-hemoproteins: HRP and CPO, both of which form quasi-stable Cpd I, along with isolated hemoglobin (Hb) chains, α and β. Examinations of the trapped primary products of 77 K cryoreduction provide insight into structural features of the parent oxy complexes in the solution state and highlight discrepancies between the actual structures of solution oxy-complexes and the structures that are visualized in crystals. Whether the primary product is the peroxo or hydroperoxoferric state, during annealing *all* proteins relax to a hydroperoxo form, which converts to Cpd I. In the case of β chains at high pH, Cpd I accumulates and is directly characterized by the spectroscopic tools employed. In all other cases, Cpd I forms but does not accumulate. A follow-up cryoreduction instead shows that when this state does not accumulate or is not captured by reaction with a bound substrate, it is reduced by redox-active products of cryoradiolysis to EPR-silent (S = 1) Cpd II, which does accumulate.

MATERIALS AND METHODS

Horseradish peroxidase (type XII, RZ 3.4), glycerol, d_3-glycerol, D_2O, and dithionate were purchased from Sigma-Aldrich. Oxy-α- and -β-chains of human hemoglobin were isolated as described previously.[32] Chloroperoxidase from the fungi *Caldariomyces fumago* (CPO) was prepared as described.[33] Complexes of ferrous horseradish peroxidase and ferrous CPO with O_2 were prepared as previously described.[34−36] Cpd II of horseradish peroxidase and CPO were prepared as described previously.[37] All protein samples were prepared in 20%−50% glycerol/buffer mixtures. Protein concentrations in the samples varied from 0.5 mM (Hrp and CPO) to 1−2 mM (globins).

γ-Irradiation of the frozen hemoprotein solutions at 77 K was performed typically for 16−20 h (dose rate of 0.15 Mrad/h, total dose 3 Mrad) using a Gamma cell 220 ^{60}Co irradiator. Annealing at multiple temperatures over the range 77−270 K was performed by placing the EPR sample in the appropriate bath (*n*-pentane or methanol cooled with liquid nitrogen) and then refreezing in liquid nitrogen. γ-Irradiation at 77 K yields an intense EPR signal at g = 2.0 from radiolytically generated organic radicals; such signals are truncated in the reported spectra. In addition, γ-irradiation produces hydrogen atoms within the fused silica tubes, and these give a characteristic hyperfine doublet with $A(^1H) \approx 507$ G. As seen in all cases, as the annealing temperature is raised, radical recombination occurs and both the radical and H atom signals decrease.

EPR/ENDOR Spectroscopy. Continuous wave (CW) EPR and ENDOR spectra were collected at Q-band (35 GHz; 2 K); X-band (variable temperature) CW EPR spectra were also collected. X-band CW EPR spectra were recorded on a Bruker ESP 300 spectrometer equipped with an Oxford Instruments ESR 910 continuous He flow cryostat. CW 35 GHz (Q-band) EPR/ENDOR spectra were recorded on a modified Varian E-109 spectrometer described previously.[2,5−7,9,10,38] All CW 35 GHz EPR/ENDOR spectra were recorded at 2 K in dispersion mode, under "rapid passage" conditions, which gives absorption line shape.[2] Derivative spectra were obtained numerically using the program LabCalc. The Q-band measurements yield better signal-to-noise ratio (S/N) and a better dispersion of g values for characterization of EPR-active centers. The X-band were optimal for cryoannealing measurements. Asymmetry in the ^{1}H ENDOR spectra commonly seen in the ENDOR spectra of cryoreduced oxyferrous hemoproteins is due to the effects of spin relaxation.[39]

dx.doi.org/10.1021/bi500296d | *Biochemistry* 2014, 53, 4894−4903

The EPR signals of cryogenerated Fe(III) species were quantitated using the corresponding resting ferric hemoproteins as standards. For spin quantitation of low-spin ferric heme species, 0.5 mM solutions of low spin myoglobin (Mb) at pH 9 and 1 mM $Cu(NO_3)_2$ were used. A solution of high-spin metMb (1 mM) in 0.1 M potassium phosphate (KPi, pH 6) or 0.5 mM ferric HRP (pH 7.0) were applied as standards for quantitation of EPR signals from high-spin ferric heme species. For determination of the amounts of Cpd II formed during decay of hydroperoxoferric intermediates, 0.5 mM solutions of corresponding compound II irradiated with the same dose were used.

RESULTS

Horseradish Peroxidase. Figure 1 and Figure S1, Supporting Information, present EPR spectra of oxyferrous HRP in 50% glycerol/buffer (pH 7), taken directly upon radiolytic cryoreduction at 77 K and after progressive annealing at temperatures above 77 K. The initial EPR spectrum after cryoreduction exhibits two EPR signals, with **g** = [2.32, 2.18, 1.94] (signal A) and [2.28, 2.16, ~1.96] (signal B) as reported previously (Table 1).[22,30,34,36] The relative intensities of the signals change in the presence of thioanisole (Figure S2, Supporting Information) but are independent of pH within the range employed, 7–8.5, and of solvent deuteration (not shown).

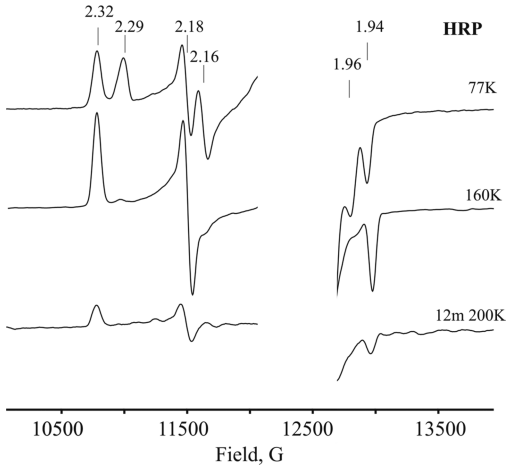

Figure 1. EPR spectra (2 K, 35 GHz) of cryoreduced oxy-HRP in 50% glycerol/0.1 mM KPi buffer, pH 7.4, and after annealing at 160 K for 1 min and at 200 K for 12 min. Instrumental conditions: T = 2 K; modulation amplitude, 2 G; microwave frequency, 34.95 GHz.

The generation of two spectroscopically distinct products from cryoreduction of oxy-HRP is indicative that the oxyferrous precursor exists in two major conformational substates. Progressive stepwise annealing up to 170 K results in conversion of B to A, as evidenced by a decay of the B signal and increase in that of A. (Figure 1; Figure S1, Supporting Information). Species A is assigned to the hydroperoxo ferriheme state[1−3] from its characteristic **g**-tensor. However, the g_{max} of species B falls between the expected maximum g-value for peroxo (g_{1max} = 2.27) and minimal value for hydroperoxo (2.28) ferriheme centers, preventing a simple assignment of this center.

To assign species B, we employed 35 GHz ^{1}H ENDOR spectroscopy. It was previously shown that the proton of a ferriheme hydroperoxo ligand exhibits an exchangeable ^{1}H ENDOR signal with maximum hyperfine coupling $A_{max} \leq 12$ MHz, $a_{iso} \approx 0.5-4$ MHz,[2,3,28] whereas ^{1}H ENDOR spectra of a peroxo species frequently exhibit more strongly coupled signals from an H-bond to the peroxo ligand, $A_{max} \approx 14-18$ MHz, $a_{iso} \approx 8-11$ MHz.[28,32] Species A was isolated for study by annealing the cryoreduced samples at 170 K, and a 2D field–frequency pattern of ^{1}H ENDOR spectra collected across its EPR envelope was prepared. The most strongly coupled ^{1}H ENDOR signal of species A was an exchangeable proton with $A_{max} \cong 8$ MHz (Figure 2); simulations of the 2D pattern were best fit with a nearly axial hyperfine tensor, $a_{iso} \cong 0.4$ MHz and $2T \cong 8.8$ MHz, (Figure S3, Supporting Information) characteristic of a hydroperoxo ferriheme, as expected. The ^{1}H ENDOR pattern of species B could then be visualized through spectroscopic differences when both were present. This 2D "sum" pattern with A and B present does not show ^{1}H

Table 1. EPR Paramaters of Cryoreduced Oxyperoxidases and Oxyglobins

protein	T_{an} (K)	g_1	g_2	g_3
oxy-HRP A	77	2.32	2.18	1.94
oxyHrp B	77	2.28	2.16	1.96
oxyCPO A	77	2.27	2.166	*a*
oxyCPO B	77	2.28	2.176	1.945
oxy β-chain (pH 8.2)	77	2.253	2.148	1.965
	190	2.31	2.19	1.946
Cpd I	215	3.24	3.24	~1.99
oxy α-chain (pH 8.2)				
A	77	2.26	2.157	~1.97
B	77	2.226	2.135	*a*
	200	2.32	2.19	1.95
oxy Mb (pH 8.2) (ref 35)	77	2.26	2.12	1.967
	190	2.31	2.185	1.93

[a]Not determined.

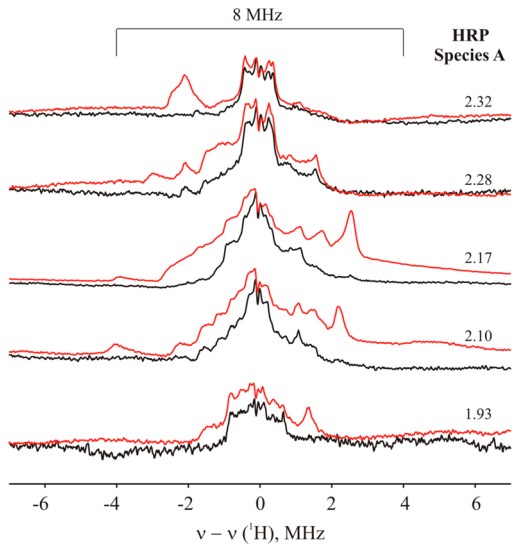

Figure 2. Two-dimensional frequency/field 35 GHz ^{1}H CW ENDOR spectra of cryoreduced oxy-HRP in 50% glycerol/H_2O buffer, pH 7.4 (red), and in 50% d_3-glycerol/D_2O buffer, pH 7 (black), annealed at 170 K for 1 min (species A). Instrumental conditions: T = 2 K, modulation amplitude, 2 G; rf power, 5 W; scan rate, 1 MHz/s; frequency bandwidth, 60 kHz; average of 20 scans; microwave frequency, 34.99 GHz.

dx.doi.org/10.1021/bi500296d | *Biochemistry* 2014, 53, 4894–4903

ENDOR intensity, A_{max}, larger than that of species A, as required if species B were a peroxoferric form, and the difference between ^{1}H ENDOR spectra of cryoreduced oxyferrous HRP containing both species A and B and those with species A only (Figure S4, Supporting Information) was similar to the pattern for species A. We thus conclude that species B also is a hydroperoxoferric heme center. The conversion of B into A during annealing then indicates that B is generated in a conformation of the hydroperoxoferriheme that is metastable in its protein environment and that this conformation relaxes to the more stable A form at temperatures as low as ∼160 K.

Upon further annealing, species A completely decays after being held at 210 K for 1 min (Figure S1, Supporting Information), but this process is accompanied by the appearance of a weak high-spin (S = 5/2) EPR signal from ferric HRP with (g-values of 6.27, 5.02) that is shown by spin quantitation versus ferric HRP to account for less than 30% of the hydroperoxoferric intermediate A, suggesting that species A primarily converts into an EPR-silent heme form. This is confirmed by the observation that a followup cryoreduction of the EPR-silent product that forms by decay of the hydroperoxy species A generates a new EPR-active center with g_{max} = 2.63, characteristic of cryoreduced HRP Cpd II.[37] (Figure 3). Spin

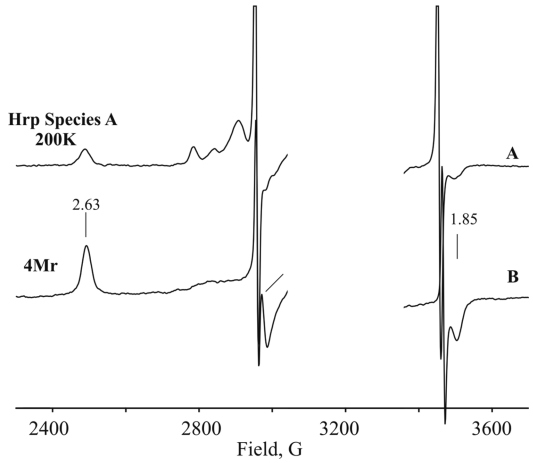

Figure 3. EPR spectra of cryoreduced oxy-HRP annealed at 210 K (complete decay of species A) (A) and 0.5 mM Cpd II of HRP (B) exposed to γ-irradiation at 77 K with dose of 4 Mr. Instrumental conditions: T = 77 K; microwave power, 20 mW; modulation amplitude, 10 G; microwave frequency, 9.092 GHz.

quantitation of this g_{max} = 2.63 signal versus that for 0.5 mM HRP Cpd II irradiated with the same dose showed that approximately 70% of species A converted into Cpd II. That Cpd II is formed from species A and not by a side reaction of ferric HRP with radiolytically generated H_2O_2 is established by the finding that Cpd II is not produced by a second irradiation of cryoreduced ferric HRP annealed at 210 K.

Formation of Cpd II as a main product during decay of hydroperoxo species A can be accounted for either by homolytic cleavage of the O−O bond of the hydroperoxo ligand or by proton-assisted heterolytic cleavage of this bond with formation of Cpd I, followed by its reduction with redox-active products of radiolysis. The decay of species A shows a strong solvent kinetic isotope effect (sKIE), slowing in D_2O/d_3-glycerol at 200 K by a factor of ∼3.5 (Figure S5, Supporting Information), which support the latter idea, with Cpd I as the primary product of proton-assisted heterolytic cleavage of the hydroperoxoferric HRP intermediate, in agreement with the known formation of this intermediate during pulsed radiolysis of oxy-HRP at room temperatures and subsequent to radiolytic cryoreduction of crystals of oxy-HRP at low temperatures.[15,23]

Formation of small amounts of high-spin ferric HRP during relaxation of the hydroperoxy intermediate may be explained either by subsequent reduction of Cpd II by products of radiolysis, or by proton-assisted dissociation of the Fe(III)−OOH species; the available data do not distinguish between these mechanisms. Regardless, the results thus suggest that the main pathway for decay of the hydroperoxoferric HRP at low temperatures, 180−200 K, proceeds through heterolytic cleavage of the O−O bond of heme-bound hydroperoxide, to form Cpd I.

CPO. UV−visible (UV−vis) absorption spectra of oxyferrous CPO radiolytically reduced in frozen solution at 77 K[21] and in crystal at 90 K[40] were reported previously but could not unambiguously establish the nature of the primary product because the absorption spectra of peroxo and hydroperoxo species are similar;[40] however, they did not detect accumulation of the relatively stable ferryl intermediates during annealing of cryoreduced oxyferrous CPO.[21] The crystal structure of cryoreduced oxy-CPO indicated that the primary species trapped at 90 K is a hydroperoxy rather than peroxy ferriheme intermediate.[40] We have used cryoreduction EPR/ENDOR spectroscopic methods to check for the primary product of reduction of oxyferrous CPO in frozen solution to reveal the mechanism of reaction of this primary product during annealing, comparing these results to the comparable ones for HRP.

The EPR spectrum of 77 K cryoreduced oxyferrous CPO (Figure 4; Figure S6, Supporting Information) again gives evidence of being an overlap of two signals, but in contrast to HRP, they are barely resolved, with both having $g_1 \approx 2.27$ (Table 1); stepwise annealing up to 190 K results in decay of one signal (A) with a concomitant increase in the intensity of the second (B) (Figure 4; Figure S6, Supporting Information). The g-tensors of A and B lie on the boundary between those

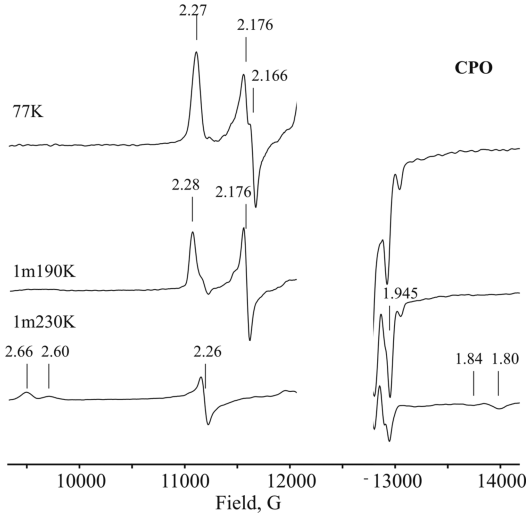

Figure 4. EPR spectra (2 K, 35 GHz) of cryoreduced oxyferrous CPO in 50% ethylene glycol/0.1 M KPi buffer, pH 4.6, and after annealing at 190 and 230 K for 1 min Instrumental conditions: as in Figure1 except microwave frequency, 35.226 GHz.

dx.doi.org/10.1021/bi500296d | Biochemistry 2014, 53, 4894−4903

for the peroxoferric and hydroperoxoferric states, but the distinction between the two can be made with ^{1}H ENDOR measurements. Figures 5 and 6 present ^{1}H ENDOR spectra of

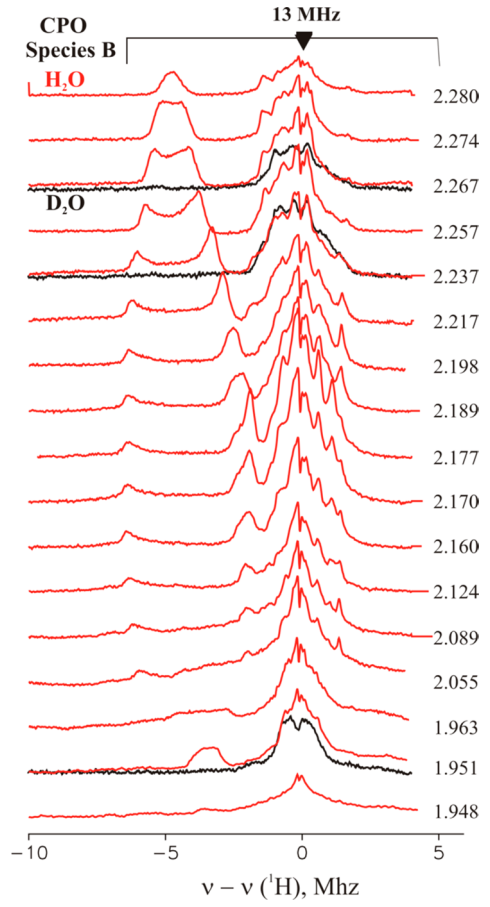

Figure 5. Two-dimensional frequency/field 35 GHz ^{1}H CW ENDOR spectra of cryoreduced ferrous oxy complex of CPO in 50% ethylene glycol/0.1 M KPi (pH 4.6) (red) and in d_2-ethylene glycol/D_2O buffer (pH 4.2) (black) annealed at 170 K for 1 min (species B). Instrumental conditions: as in Figure2.

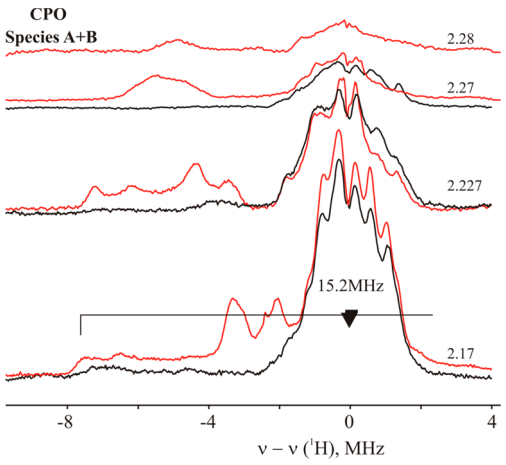

Figure 6. Two-dimensional frequency/field 35 GHz ^{1}H CW ENDOR spectra of cryoreduced ferrous oxy complex of CPO in 50% ethylene glycol/0.1 M KPi (species A + B; pH 4.6) (red) and in d_2-ethylene glycol/D_2O buffer (pH 4.2) (black). Instrumental conditions as in Figure2.

cryoreduced oxy-CPO containing species A and B and a sample annealed at 170 K, which contains only species B. Species B shows an exchangeable proton signal with A_{max} = 13 MHz (Figure 5). Simulations of the 2D field-frequency pattern of ENDOR spectra collected across the EPR envelope of species B lead to the best fit that employed a nearly axial hyperfine tensor with $a_{iso} \cong 0.4$ MHz and $T \cong 4.4$ MHz (not shown), characteristic of a hydroperoxo ligand proton.[2,3] ^{1}H ENDOR spectra of cryoreduced oxyferrous CPO consisting of species A and B are a superposition of the ^{1}H signal from species B, plus the signal from an additional, more strongly coupled exchangeable proton from species A with larger $A_{max} \approx 15$ MHz (Figure 6), characteristic of a hydrogen bond to a peroxo ligand.[28,32] Species A and B thus can be assigned to peroxo and hydroperoxoferric intermediates, respectively; during annealing at 140−170 K, the peroxo intermediate A is protonated to form the hydroperoxo species B.

These results indicate that there are two conformers of the oxy-heme in the oxyferrous CPO parent, as is the case for oxyferrous HRP, but that with CPO, 77 K cryoreduction of one conformer generates a peroxoferriheme species that accepts a proton at 77 K to form a hydroperoxy ferriheme species B, whereas the peroxoferric species A in the second conformer remains unprotonated. Only through cryoannealing at $T > 140$ K does the CPO heme center relax so that the peroxoferric conformer A can acquire a proton and convert to the hydroperoxoferric state. In contrast, both conformers in oxy-HRP acquire a proton at 77 K upon cryoreduction.

The hydroperoxoferric CPO intermediate B completely decays after further annealing at 200 K for 10 min (Figure 4). This process occurs without accumulation of Cpd I and with only ∼30% converting to low-spin ferric CPO,[41] (species with **g** = [2.66, 2.26, 1.80] and [2.60, 2.26, 1.84]). Instead the majority of B converts to an EPR-silent product state. Cryoreduction of this EPR-silent product creates the EPR-active center with g_{max} = 2.42, characteristic of cryoreduced CPO Cpd II (Figure S7, Supporting Information).[37] Thus, as above for hydroperoxyferric HRP, Cpd II is the main product of annealing of cryogenerated hydroperoxyferric CPO.

Oxy-*α*- and -*β*-Chains of HbA. It was previously shown that multiple peroxoferric species are produced during 77 K radiolytic reduction of oxy-*α*- and oxy-*β*-chains,[30,32,42] and we reported detailed EPR and ENDOR analysis of these species.[32] The cryogenerated peroxoferric species convert into hydroperoxy ferric intermediates upon annealing at temperatures above 170 K, and these in turn decay completely at temperatures within the range of 200−230 K.[8,30,42] We recently showed that during annealing of cryoreduced oxyferrous Mb, EPR silent (S = 1) Cpd II is formed, as detected by Mossbauer spectroscopy,[8] thus correcting the early suggestion that the decay of the hydroperoxoferric intermediate forming during annealing of cryoreduced oxy ferrous *α*- and *β*-chains and oxyferrous Mb proceeds via dissociation of the hydroperoxo ligand.[30,42] Because the Cpd II is presumably formed by conversion of the hydroperoxoferric state to Cpd I, which then is reduced by radicals formed by the cryoradiolysis, we have reexamined the annealing of cryoreduced oxyferrous *α*- and *β*-chains to see if the Cpd I state could be observed directly.

As shown in Figure 7, cryoreduction of oxyferrous *β*-chains produces as primary product the peroxoferric state; annealing at 165 K converts this to two new peroxo intermediates; further annealing at 180−190 K converts the peroxo intermediates to a hydroperoxo ferriheme state with characteristic **g** = [2.303,

dx.doi.org/10.1021/bi500296d | Biochemistry 2014, 53, 4894−4903

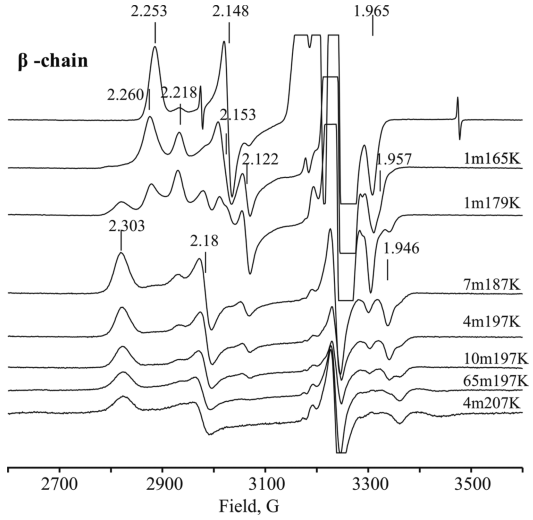

Figure 7. CW EPR (77 K) spectra of cryoreduced 1 mM oxy-β-chain HbA in 16% glycerol/buffer, pH 8.2, annealed at indicated conditions. Instrumental conditions: t = 28 K, modulation amplitude, 5 G; microwave frequency, 9.101 GHz.

2.18, 1.946]. This assignment is supported by ^{1}H ENDOR data, presented in Figure S8, Supporting Information, which exhibits a strongly coupled doublet, exchangeable in D_2O, with A_{max} = 12 MHz, characteristic of the hydroperoxy ligand.[2−4] The maximum accumulation of the hydroperoxy intermediate during annealing of cryoreduced oxyferrous β-chains was noticeably higher at pH 8 than at pH 7 (Figure S9, Supporting Information), and this species is almost undetectable at pH 6 (Figure S10, Supporting Information). This decrease in accumulation is caused by an increased rate of proton-assisted decay of the hydroperoxo species at low pH, as seen during annealing of cryoreduced oxy ferrous DHP and during the reaction of metMb with H_2O_2 at ambient temperature.[28,43]

In contrast to the behavior of HRP and CPO, the hydroperoxy intermediate of β-chain formed at pH 8.2 decays upon annealing at temperatures above 200 K to a new EPR-active state that can be assigned to Cpd I. It exhibits an axial EPR signal that can be detected without noticeable broadening only at temperatures below 16 K (Figure 8), with $g_\perp$ = 3.24, $g_\parallel \approx 2$. This species exhibits ^{1}H ENDOR signals from two

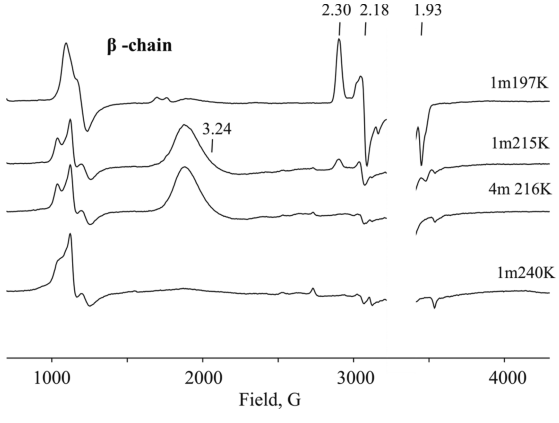

Figure 8. X-band EPR spectra of cryoreduced oxy complex of β chains (16% glycerol/0.05 M Tris buffer, pH 8.2) annealed at indicated conditions. Instrumental conditions: T = 8 K; modulation amplitude, 10 G; microwave power, 10 mW; microwave frequency, 9.378 GHz.

nonexchangeable, strongly coupled protons, with maximum effective hyperfine couplings of 22 and 10 MHz at g-3.24, corresponding to intrinsic couplings of 13.6 and 6.2 MHz (Figure S11, Supporting Information). Comparison of the g-values and ^{1}H ENDOR data with properties of other Cpds I show that the g-3.24 signal arises from an S = 3/2 Cpd I in which the porphyrin π-cation radical is ferromagnetically coupled with the Fe(IV) (S = 1) heme center, as first observed with Cpd I of catalase[44] and as observed during cryoreduction/annealing experiments with the structurally similar oxyferrous DHP[28] and in clear distinction with the Cpds I of CPO and P450cam.

The kinetics of the appearance of this β-chain Cpd I (pH 8.2) measured during cryoannealing at 205 K match well with the decay of the hydroperoxoferric intermediate (Figure 9),

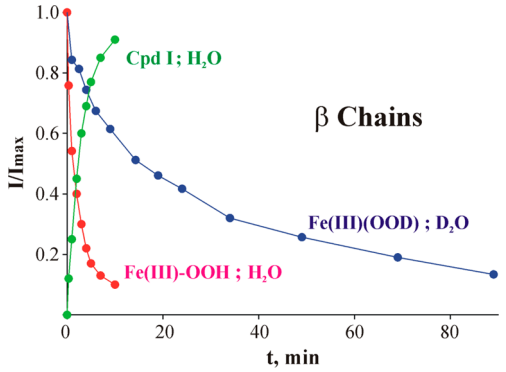

Figure 9. Kinetics of decay of hydroperoxoferric intermediate of β-chain in 16% glycerol/buffer, pH 8.13 (red), and in 16% d_3-glycerol/D_2O buffer, pH 7.73 (blue), and appearance of Cpd I (g = 3.24) in 16% glycerol/buffer, pH 8.13 (green), at 205 K.

confirming that this state is kinetically competent to directly form Cpd I. The observation of a large sKIE in the formation of Cpd I (effective solvent KIE > 6) (Figure 9) confirms that this conversion involves proton delivery to the hydroperoxoferric moiety and its subsequent heterolytic cleavage. The resulting Cpd I is less stable at low pH, with a decrease in its accumulation by almost 3-fold at pH 7 (not shown), and the stability is further decreased at pH 6 (Figure S10, Supporting Information).

At pH 8.2, the β-chain Cpd I EPR signal disappears completely upon annealing at 240 K for 1 min (Figure 8 and Figure S12, Supporting Information). This decay is accompanied by less than 25% conversion to a low-spin ferric state. Instead, the chief product again is a Cpd II intermediate formed by reduction of Cpd I during annealing, as confirmed by a second cryoreduction of the cryoannealed proteins (Figure S13, Supporting Information).[37] The intensity of the resulting cryogenerated ferriheme signal is almost independent of pH, which indicates that the yield of Cpd II is independent of pH.

Similar cryoreduction/annealing experiments carried out with oxyferrous α-chains do not yield detectable signals from a Cpd I intermediate even at pH > 8 (Figure 10; Figure S14, Supporting Information). At high pH, the final product of decay of the hydroperoxy ferric intermediate of the α-chains detected by EPR is a low-spin ferric state, which accounts for only ∼20% of cryogenerated hydroperoxy ferric intermediate. Subsequent reirradiation of the sample annealed at 230 K (Figure 10) generates a ferriheme EPR signal with g_{max} = 2.43 characteristic of cryoreduced Cpd II (Figure S13, Supporting

dx.doi.org/10.1021/bi500296d | Biochemistry 2014, 53, 4894−4903

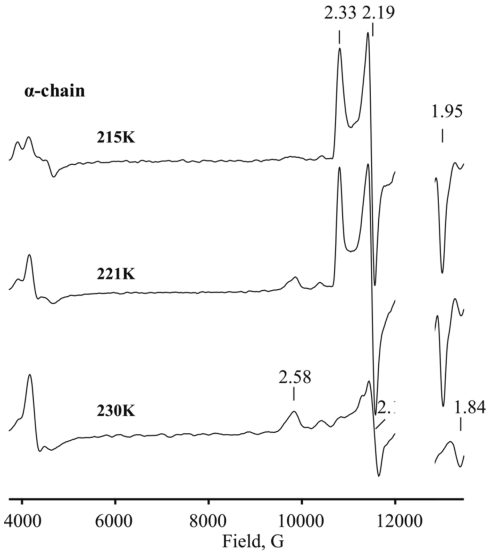

Figure 10. CW EPR spectra (2 K, 35 GHz) of cryoreduced oxy-α-chains (16% glycerol/0.05 M Tris buffer, pH 8.2) and after annealing at indicated temperatures for 1 min. Instrumental conditions: T = 2 K; amplitude modulation, 4 G; microwave frequency, 35.155 GHz.

Information). Spin quantitation of the signal shows that ~80% of the hydroperoxy ferric intermediate converted into compound II during annealing.

DISCUSSION

The present study has suggested that Cpd I is produced by the relaxation of the hydroperoxo ferriheme intermediate generated through 77 K cryoreduction of a variety of hemoproteins and explains why Cpd I nonetheless is seldom seen to accumulate in these experiments. The present studies further provide insight into the active-site structure of oxyferrous HRP and oxyferrous CPO in frozen solution.

Structural Features of Ferrous Oxy-HRP and -CPO Complexes in Frozen Solution. Cryoreduced species trapped at 77 K preserve the structure of the parent diamagnetic precursor[2,3,28,32,45] and therefore can provide sensitive EPR/ENDOR probes for studying structural features of the precursor oxyferrous heme moiety. Previously this approach was successfully applied to oxyferrous α- and β-chains of HbA,[32] oxyferrous gsNOS,[4] oxyferrous DHP,[28]and oxyferrous indoleamine 2,3-dioxygenase (IDO).[46]

The EPR and ^{1}H ENDOR data presented herein show that 77 K cryoreduction of oxyferrous HRP yields two conformers of the hydroperoxoferric species, A and B, an indication that the oxy precursor in solution exists in two conformational substates. These substate populations are independent of pH within the studied range of pH 7−8.5 and only slightly change in the presence of thioanisole. Correspondingly, two conformational substates were also reported for Cpd II of HRP.[37] In contrast, the crystal structure of oxyferrous HRP obtained at 100 K does not exhibit two conformational substates.[47] Presumably, crystallization stabilizes a single conformation of the oxy complex, as occurs during crystallization of oxyferrous Hb.[47]

Cryoreduction injects an electron to an oxy-heme, generating the peroxoferriheme moiety, yet the 77 K cryoreduction of oxyferrous HRP yields the hydroperoxoferric species, the result of electron *and* proton addition. Previous cryoreduction studies with a variety of oxy-hemoproteins, including P450, NOS, and heme oxygenase (HO), have shown that proton delivery to the reduced dioxygen formed at 77 K or below requires the presence in the parent oxy-complex of an H-bonded proton delivery network ending in an ordered water molecule that is hydrogen-bonded to the terminal oxygen of the dioxygen ligand.[1−4,28,46,48] This water mediates the proton transfer to the peroxo ligand at 77 K or below by lowering the barrier for proton transfer.[4,49−51] For example, the crystal structure of oxyferrous HRP obtained at 100 K showed that the distal oxygen is within H-bond distances to the $N^{\varepsilon}2$ atom of His42 (2.9 Å), the N^{ε} atom of Arg38 (2.9 Å), and a water molecule (2.9 Å).[29] In this case, both these residues may serve as proton donors, although the water molecule does not have optimal geometry to mediate proton transfer from the proton donors to the distal oxygen of cryogenerated peroxo ligand.

In this context, it is noteworthy that the ferryl oxygen of Cpd II of HRP becomes protonated upon cryoreduction at 77 K.[37] The crystal structure of Cpd II showed that in this case, the proton can be transferred to the reduced ferryl moiety from His42 via the intervening water molecule, which links the proton donor and acceptor by H-bonds.[29] This correspondingly suggests that unlike in the crystal, in solution an ordered molecule of water can optimize the coupling between the hydrogen bonding network and the peroxo ligand, cryogenerated in frozen solution, enabling proton transfer from the proton donor residue.

Another important distinction between cryoreduced oxyferrous HRP in frozen solution and in the crystal is that the hydroperoxy ferric intermediate (sometimes denoted, Cpd 0) does not form as one of the products of cryoreduction of oxyferrous HRP in the crystalline state,[29] even though this intermediate was trapped and characterized during cryoreduction of the crystal of oxyferrous CPO[40] and oxyferrous heme oxygenase.[15] This difference between solution and crystal HRP likely indicates that the proton delivery networks in crystal and in solution differ (see below). Finally the fact that species B of HRP trapped at 77 K converted into species A, both of which are shown above to contain a hydroperoxo ferriheme, at a relatively low annealing temperature indicates that this conversion is due to reorientation of the cryogenerated hydroperoxy ligand rather than protonation of the cryogenerated peroxo ligand as had been suggested previously.[22]

Cryoreduced oxyferrous CPO also exhibits two spectroscopically distinct species, denoted A and B (Table 1, Figure 4, and Figure S6, Supporting Information), but in this case, the ENDOR data shows that A is a peroxo ferriheme and B is a hydroperoxo ferriheme intermediate; progressive annealing at 130−160 K results in protonation of the peroxo ligand of A and its conversion to the hydroperoxy ferriheme form B (Figure S6, Supporting Information). These species and such transformations are not effectively distinguished with optical spectroscopy because they exhibit essentially indistinguishable optical spectra.[40] The presence of two distinct products of cryoreduction indicates the presence of two conformational substates in the oxyferrous CPO parent, which correlates with the observation of two conformers in CPO Cpd II.[52]

Interestingly, during radiolytic cryoreduction of oxyferrous CPO in the crystal at 100 K, only the hydroperoxy ferric heme species accumulates,[40] even though the structure does not show an ordered water molecule H-bonded to the distal oxygen that could mediate proton transfer from Glu183 to the cryogenerated peroxo ligand. Instead, the crystal structure shows that the carboxylate side chain of Glu183 is located 2.7 Å from the

dx.doi.org/10.1021/bi500296d | *Biochemistry* 2014, 53, 4894−4903

distal oxygen, poised to serve as the proton donor.[40] However, proton transfer only occurs at 77 K in conformer B of the ferrous oxy complex (B). In the alternative conformer, A, the geometry of hydrogen bonding interaction between Glu183 and distal oxygen of peroxo ligands is likely unfavorable for the proton transfer, and the peroxo-ferriheme accumulates at 77 K. Presumably, during annealing of the cryoreduced oxyferrous CPO in frozen solution at higher temperatures, small mutual reorientations of residue Glu183 and the peroxy ligand enable protonation of the latter.

As noted above, the primary products trapped during cryoreduction of crystal and frozen solution are frequently not the same, presumably because of differences in structural details of the oxyheme site in the crystalline form and in frozen solution. For instance, hydroperoxy intermediates were trapped during cryoreduction of oxy-P450 and oxy-HRP in solution, while these intermediates were not detected in crystals.[2,29,53] Instead, in a crystal of cryoreduced oxyferrous HRP, only the products of heterolytic cleavage of the O−O bond were detected, namely, Cpd I and H_2O, products that require the transfer of two protons to the cryogenerated peroxo ligand.[29] Our results show that this could not happen in the protein in frozen solution at temperatures of 100 K. Also cryoreduction of Mb Cpd II in solution and in a crystal produced different primary products.[37,54] To our knowledge, only oxyferrous Mb in crystal and frozen solution shows similar spectroscopic and relaxation properties upon cryoreduction.[30,55] The differences in the behavior of the solution and crystal upon cryoreduction are likely a consequence of structural changes in the oxyferous protein parent complexes induced by crystallization.[47] The presence of both hydroperoxoferric and peroxoferric states in cryoreduced oxyferrous CPO in frozen solution but only the hydroperoxoferric state in the crystal in part may be also due to different conditions used for preparation of oxy complexes in crystal and solution or to a relatively low resolution of the crystal structure that does not allow resolution of both conformers.

Reaction Pathways of Decay of Hydroperoxo Ferriheme Intermediates. The data presented herein show that the hydroperoxo ferriheme intermediate generated through cryoreduction/annealing of oxyferrous β chains undergoes proton-assisted conversion to Cpd I. At high pH, Cpd I accumulates and was characterized by EPR/ENDOR. Cpd I did not accumulate sufficiently to be observed by EPR during decay of the β-chain hydroperoxo ferric intermediate at lower pH, and under no conditions was Cpd I observed for HRP, CPO, α-chains, or Mb,[8] even though Cpd I of HRP and CPO are relatively stable at 200 K, the temperature at which decay of the hydroperoxy intermediates is complete. One might imagine a trivial explanation for failures to see Cpd I: proton-assisted decay of the hydroperoxoferric state occurs by protonation of the OOH- ligand and loss of H_2O_2, leaving a ferriheme product state. However, that cannot be a major reason: over 70% of the cryogenerated hydroperoxo intermediate in these proteins converted to Cpd II during this cryoannealing even without accumulation of Cpd I, and this could not happen by this mechanism.

Cpd II can instead form from the hydroperoxo ferriheme intermediate in two alternative ways: (i) by homolytic cleavage of the O−O bond of the hydroperoxo ligand, which is not a proton dependent process, (ii) by rapid reduction either of the hydroperoxo ferriheme species, or (iii) by rapid reduction of the Cpd I formed by proton-assisted heterolytic cleavage of the O−OH bond of the hydroperoxo ferriheme. Reduction of a Cpd I thus formed can involve redox-active (radical) products of radiolysis or, in the case of α-chains and Mb, which do not form a stable Cpd I, reduction by a nearby amino acid residue.[56] The present experiments do not distinguish among these alternatives.

Decay of the hydroperoxyferric intermediates for *all* the hemoproteins studied showed a strong solvent KIE, indicative of a proton-dependent decay via heterolytic cleavage of the O−O bond or dissociation of hydrogen peroxide, and this excludes mechanism i, cleavage of the O−O bond. Mechanism ii, formation of Cpd II by direct reduction of the hydroperoxo ferriheme, is unlikely, because previous studies have shown that this state is a poor oxidant.[57,58] In support of this conclusion, Cpd II was not detected during decay of the cryogenerated hydroperoxo ferric intermediate of HO, which does not form Cpd I, in contrast to Cpd I formation during annealing of hydroperoxoferric myoglobin.[8] Accordingly, the evidence indicates that mechanism iii is operative, that Cpd II forms via reduction of Cpd I; because Cpd I is stable in HRP and CPO, this reduction must involve redox-active products of radiolysis, not protein residues.

Formation of redox-active species during radiolysis was demonstrated by Denisov et al.,[10] and the EPR spectra of radical species, many of which must be redox-active, is seen for all proteins subjected to 77 K cryoreduction. These radicals disappear through recombination/electron transfer upon annealing and typically are gone after annealing for ∼1 min at ∼230 K. Thus, effective reduction of Cpd I to Cpd II is to be expected if formation of Cpd I is completed by annealing at temperatures below 200 K, since concentrations of the radiolytically generated redox-active products are still high. If conversion of the hydroperoxo ferriheme species to Cpd I does not occur until higher temperatures, then it is possible for Cpd I to accumulate, as seen for Cpd I of β-chains. In this case, at pH above 8, Cpd I forms at relatively high temperatures (>200 K, Figure 9), that is, under conditions where the concentration of radiolytically generated redox-active species is relatively low. At lower pH, proton-assisted decay of the hydroperoxo ferriheme speeds up and occurs at lower temperatures, where the redox-active radical species remain in high concentration. The decreased yield of Cpd I at low pH thus may be attributed to more effective reduction of Cpd I, possibly along with its lower intrinsic stability. Interestingly, the only Cpds I that have been trapped in this way are ferromagnetically coupled, with $S = 3/2$. It may be that the $S = 1/2$ Cpd I seen for HRP and CPO (and possibly Mb and α-chains) has higher reactivity with radiolytically generated redox-active radicals.

The above presentation shows that during cryoannealing the majority of the hydroperoxy ferric intermediate converts to Cpd I, which in general is reduced to Cpd II by radiolytically generated radicals. Although Cpd II is stable at 200 K, at this annealing temperature, we also see the formation of small amounts of ferriheme states. Most likely these are formed through reduction of Cpd II by radicals, but it is also possible that there is a contribution from a small amount of dissociation of HOOH.

SUMMARY

(i) The data presented here suggest that the hydroperoxoferric intermediates formed subsequent to 77 K radiolytic cryoreduction of oxyferrous hemoproteins in general relax to Cpd I during cryoannealing, unless this state first reacts with substrate.

dx.doi.org/10.1021/bi500296d | *Biochemistry* 2014, 53, 4894−4903

This finding, based on EPR/ENDOR analysis, revises current views about the mechanism of decay of the hydroperoxoferric state at low temperature via dissociation of H_2O_2. (ii) We further show that when Cpd I is not captured by substrate, in general it does not accumulate in cryoreduction experiments because it is reduced to Cpd II by redox-active products of radiolysis. (iii) Comparative analysis of cryoreduced ferryl and oxyferrous hemoproteins in crystal form and in frozen solution indicates that crystallization can often cause structural changes in the active site.

■ ASSOCIATED CONTENT

Supporting Information

EPR and ENDOR spectra and KIE analysis. This material is available free of charge via the Internet at http://pubs.acs.org.

■ AUTHOR INFORMATION

Corresponding Authors

*Brian M. Hoffman. Phone: 847-491-3104. Fax: 847-491-7713. E-mail: bmh@northwestern.edu.

*John H. Dawson. Phone: 803-777-7234. Fax: 803-777-9521. E-mail: dawson@sc.edu.

Funding

This work was supported by the NIH (Grant GM 111097, B.M.H.) and NSF (Grant MCB 0820456, J.H.D.).

Notes

The authors declare no competing financial interest.

■ ACKNOWLEDGMENTS

We thank Prof. Lowell P. Hager (deceased) for providing the *C. fumago* chloroperoxidase. We acknowledge Prof. H. Halpern for access to the Gammacell 220 irradiator.

■ ABBREVIATIONS

HRP, horseradish peroxidase; CPO, chloroperoxidase; DHP, dehaloperoxidase; NOHA, N^{ω}-hydroxy-L-arginine; CW, continuous wave

■ REFERENCES

(1) Davydov, R., and Hoffman, B. M. (2011) Active intermediates in heme monooxygenase reactions as revealed by cryoreduction/annealing, EPR/ENDOR studies. *Arch. Biochem. Biophys. 507*, 36−43.

(2) Davydov, R., Makris, T. M., Kofman, V., Werst, D. W., Sligar, S. G., and Hoffman, B. M. (2001) Hydroxylation of Camphor by Reduced oxy-Cytochrome P450cam: Mechanistic Implications of EPR and ENDOR of Catalytic Intermediates in Native and Mutant Enzymes. *J. Am. Chem. Soc. 123*, 1403−1415.

(3) Davydov, R., Kofman, V., Fujii, H., Yoshida, T., Ikeda-Saito, M., and Hoffman, B. (2002) Catalytic Mechanism of Heme Oxygenase through EPR and ENDOR of Cryoreduced Oxy-Heme Oxygenase and Its Asp140 Mutants. *J. Am. Chem. Soc. 124*, 1798−1808.

(4) Davydov, R., Sudhamsu, J., Lees, N. S., Crane, B. R., and Hoffman, B. M. (2009) EPR and ENDOR Characterization of the Reactive Intermediates in the Generation of NO by Cryoreduced Oxy-Nitric Oxide Synthase from *G. stearothermophilus*. *J. Am. Chem. Soc. 131*, 14493−14507.

(5) Davydov, R., Dawson, J. H., Perera, R., and Hoffman, B. M. (2013) The use of deuterated camphor as a substrate in (1)H ENDOR studies of hydroxylation by cryoreduced oxy P450cam provides new evidence of the involvement of compound I. *Biochemistry 52*, 667−671.

(6) Davydov, R., Gilep, A. A., Strushkevich, N. V., Usanov, S. A., and Hoffman, B. M. (2012) Compound I Is the Reactive Intermediate in the First Monooxygenation Step during Conversion of Cholesterol to Pregnenolone by Cytochrome P450scc: EPR/ENDOR/Cryoreduction/Annealing Studies. *J. Am. Chem. Soc. 134*, 17149−17156.

(7) Davydov, R., Razeghifard, R., Im, S.-C., Waskell, L., and Hoffman, B. M. (2008) Characterization of the Microsomal Cytochrome P450 2B4 O2-Activation Intermediates by Cryoreduction/EPR. *Biochemistry 47*, 9661−9666.

(8) Garcia-Serres, R., Davydov, R. M., Matsui, T., Ikeda-Saito, M., Hoffman, B. M., and Huynh, B. H. (2007) Distinct Reaction Pathways Followed upon Reduction of Oxy-Heme Oxygenase and Oxy-Myoglobin as Characterized by Moessbauer Spectroscopy. *J. Am. Chem. Soc. 129*, 1402−1412.

(9) Davydov, R., Perera, R., Jin, S., Yang, T.-C., Bryson, T. A., Sono, M., Dawson, J. H., and Hoffman, B. M. (2005) Substrate Modulation of the Properties and Reactivity of the Oxy-Ferrous and Hydroperoxoferric Intermediates of Cytochrome P450cam as Shown by Cryoreduction- EPR/ENDOR Spectroscopy. *J. Am. Chem. Soc. 127*, 1403−1413.

(10) Denisov, I. G., Makris, T. M., and Sligar, S. G. (2001) Cryotrapped reaction intermediates of cytochrome P450 studied by radiolytic reduction with phosphorus-32. *J. Biol. Chem. 276*, 11648−11652.

(11) Ortiz de Montellano, P. R. (2010) Hydrocarbon hydroxylation by cytochrome P 450 enzymes. *Chem. Rev. 110*, 932−948.

(12) Hamdane, D., Zhang, H., and Hollenberg, P. (2008) Oxygen activation by cytochrome P450 monooxygenase. *Photosynth Res. 98*, 657−666.

(13) Poulos, T. L. (2005) Structural biology of heme monooxygenases. *Biochem. Biophys. Res. Commun. 338*, 337−345.

(14) Ortiz de Montellano, P. R., Ed. (2004) *Cytochrome P450: Structure, Mechanism, and Biochemistry*, 3rd ed., Kluwer Academic/Plenum Publishers, New York.

(15) Matsui, T., Iwasaki, M., Sugiyama, R., Unno, M., and Ikeda-Saito, M. (2010) Dioxygen Activation for the Self-Degradation of Heme: Reaction Mechanism and Regulation of Heme Oxygenase. *Inorg. Chem. 49*, 3602−3609.

(16) Marletta, M. A., Hurshman, A. R., and Rusche, K. M. (1998) Catalysis by nitric oxide synthase. *Curr. Opin. Chem. Biol. 2*, 656−663.

(17) Zhu, Y., and Silverman, R. B. (2008) Revisiting Heme Mechanisms. A Perspective on the Mechanisms of Nitric Oxide Synthase (NOS), Heme Oxygenase (HO), and Cytochrome P450s (CYP450s). *Biochemistry 47*, 2231−2243.

(18) Davydov, R., Matsui, T., Fujii, H., Ikeda-Saito, M., and Hoffman, B. M. (2003) Kinetic Isotope Effects on the Rate-Limiting Step of Heme Oxygenase Catalysis Indicate Concerted Proton Transfer/Heme Hydroxylation. *J. Am. Chem. Soc. 125*, 16208−16209.

(19) Ortiz de Montellano, P. R., and Wilks, A. (2001) Heme Oxygenase Structure and Mechanism. *Adv. Inorg. Chem. 51*, 359−407.

(20) Matsui, T., Unno, M., and Ikeda-Saito, M. (2010) Heme oxygenase reveals its strategy for catalyzing three successive oxygenation reactions. *Acc. Chem. Res. 43*, 240−247.

(21) Denisov, I. G., Dawson, J. H., Hager, L. P., and Sligar, S. G. (2007) The ferric-hydroperoxo complex of chloroperoxidase. *Biochem. Biophys. Res. Commun. 363*, 954−958.

(22) Denisov, I. G., Makris, T. M., and Sligar, S. G. (2002) Formation and Decay of Hydroperoxo-Ferric Heme Complex in Horseradish Peroxidase Studied by Cryoradiolysis. *J. Biol. Chem. 277*, 42706−42710.

(23) Kobayashi, K., and Hayashi, K. (1981) One-electron reduction in oxyform of hemoproteins. *J. Biol. Chem. 256*, 12350−12354.

(24) Kim, S. H., Perera, R., Hager, L. P., Dawson, J. H., and Hoffman, B. M. (2006) Rapid freeze-quench ENDOR study of chloroperoxidase compound I: the site of the radical. *J. Am. Chem. Soc. 128*, 5598−5599.

(25) Spolitak, T., Funhoff, E. G., and Ballou, D. P. (2010) Spectroscopic studies of the oxidation of ferric CYP153A6 by peracids: Insights into P450 higher oxidation states. *Arch. Biochem. Biophys. 493*, 184−191.

(26) Spolitak, T., Dawson, J. H., and Ballou, D. P. (2008) Replacement of tyrosine residues by phenylalanine in cytochrome

P450cam alters the formation of Cpd II-like species in reactions with artificial oxidants. *JBIC, J. Biol. Inorg. Chem. 13*, 599−611.
(27) Rittle, J., and Green, M. T. (2010) Cytochrome P450 compound I: Capture, characterization, and C-H bond activation kinetics. *Science 330*, 933−937.
(28) Davydov, R., Osborne, R., Shanmugam, M., Du, J., Dawson, J., and Hoffman, B. (2010) Probing the oxyferrous and catalytically active ferryl states of *Amphitrite ornata* dehaloperoxidase by cryoreduction and EPR/ENDOR spectroscopy. Detection of Compound I. *J. Am. Chem. Soc. 132*, 14995−15004.
(29) Berglund, G. I., Carlsson, G. H., Smith, A. T., Szoeke, H., Henriksen, A., and Hajdu, J. (2002) The catalytic pathway of horseradish peroxidase at high resolution. *Nature 417*, 463−468.
(30) Kappl, R., Höhn-Berlage, M., Hüttermann, J., Bartlett, N., and Symons, M. C. R. (1985) Electron spin and electron nuclear-double resonance of the $[FeO_2]^-$ centre from irradiated oxyhemo- and oxymyoglobin. *Biochim. Biophys. Acta 827*, 327−343.
(31) Jung, C., de Vries, S., and Schunemann, V. (2011) Spectroscopic characterization of cytochrome P450 Compound I. *Arch. Biochem. Biophys. 507*, 44−55.
(32) Davydov, R., Kofman, V., Nocek, J., Noble, R. W., Hui, H., and Hoffman, B. M. (2004) Conformational Substates of the Oxyheme Centers in a and b Subunits of Hemoglobin as Disclosed by EPR and ENDOR Studies of Cryoreduced Protein. *Biochemistry 43*, 6330−6338.
(33) Blanke SR, Y. S., and Hager, L. P. (1989) Development of semi-continuous and continuous flow bioreactors for the high level production of chloroperoxidase. *Biotechnol. Lett. 11*, 769−774.
(34) Davydov, R. M., and Khangulov, S. V. (1983) ESR spectroscopy of unstable intermediates of the reduction of oxygen complexes of cytochrome P 450 and other hemoproteins. *Stud. Biophys. 95*, 97−106.
(35) Sono, M., Eble, K. S., Dawson, J. H., and Hager, L. P. (1985) Preparation and properties of ferrous chloroperoxidase complexes with dioxygen, nitric oxide, and an alkyl isocyanide. Spectroscopic dissimilarities between the oxygenated forms of chloroperoxidase and cytochrome P-450. *J. Biol. Chem.*, 15530−15535.
(36) Gasyna, Z. (1979) Intermediate spin-states in one-electron reduction of oxygen-hemoprotein complexes at low temperature. *FEBS Lett. 106*, 213−218.
(37) Davydov, R., Osborne, R. L., Kim, S.-H., Dawson, J. H., and Hoffman, B. M. (2008) EPR and ENDOR Studies of cryoreduced Compounds II of peroxidases and myoglobin. Proton-coupled electron transfer and Protonation status of ferryl hemes. *Biochemistry 47*, 5147−5155.
(38) Kim, S. H., Yang, T.-C., Perera, R., Jin, S., Bryson, T. A., Sono, M., Davydov, R., Dawson, J. H., and Hoffman, B. M. (2005) Cryoreduction EPR and 13C, 19F ENDOR study of substrate-bound substates and solvent kinetic isotope effects in the catalytic cycle of cytochrome P450cam and its T252A mutant. *Dalton Trans. 21*, 3464−3469.
(39) Epel, B., Poppl, A., Manikandan, P., Vega, S., and Goldfarb, D. (2001) The Effect of Spin Relaxation on ENDOR Spectra Recorded at High Magnetic Fields and Low Temperatures. *J. Magn. Reson. 148*, 388−397.
(40) Kuhnel, K., Derat, E., Terner, J., Shaik, S., and Schlichting, I. (2007) Structure and quantum chemical characterization of chloroperoxidase compound 0, a common reaction intermediate of diverse heme enzymes. *Proc. Natl. Acad. Sci. U.S.A. 104*, 99−104.
(41) Hollenberg, P. F., Hager, L. P., Blumberg, W. E., and Peisach, J. (1980) An electron paramagnetic resonance study of the high and low spin forms of chloroperoxidase. *J. Biol. Chem. 256*, 4801−4807.
(42) Symons, M. C. R., and Petersen, R. L. (1978) Electron capture by Oxyhaemoglobin: an e.s.r. study. *Proc. R. Soc. London, Ser. B 201*, 285−300.
(43) Egawa, T., Yoshioka, S., Takahashi, S., Hori, H., Nagano, S., Shimada, H., Ishimori, K., Morishima, I., Suematsu, M., and Ishimura, Y. (2003) Kinetic and Spectroscopic Characterization of a Hydroperoxy Compound in the Reaction of Native Myoglobin with Hydrogen Peroxide. *J. Biol. Chem. 278*, 41597−41606.
(44) Benecky, M. J., Frew, J. E., Scowen, N., Jones, P., and Hoffman, B. M. (1993) EPR and ENDOR detection of compound I from *Micrococcus lysodeikticus* catalase. *Biochemistry 32*, 11929−11934.
(45) Unno, M., Chen, H., Kusama, S., Shaik, S., and Ikeda-Saito, M. (2007) Structural Characterization of the Fleeting Ferric Peroxo Species in Myoglobin: Experiment and Theory. *J. Am. Chem. Soc. 129*, 13394−13395.
(46) Davydov, R. M., Chauhan, N., Thackray, S. J., Anderson, J. L. R., Papadopoulou, N. D., Mowat, C. G., Chapman, S. K., Raven, E. L., and Hoffman, B. M. (2010) Probing the Ternary Complexes of Indoleamine and Tryptophan 2,3-Dioxygenases by Cryoreduction EPR and ENDOR Spectroscopy. *J. Am. Chem. Soc. 132*, 5494−5500.
(47) Wilson, S. A., Green, E., Mathews, I. I., Benfatto, M., Hodgson, K. O., Hedman, B., and Sarangi, R. (2013) X-ray absorption spectroscopic investigation of the electronic structure differences in solution and crystalline oxyhemoglobin. *Proc. Natl. Acad. Sci. U.S.A. 110*, 16333−16338.
(48) Davydov, R., Chemerisov, S., Werst, D. E., Rajh, T., Matsui, T., Ikeda-Saito, M., and Hoffman, B. M. (2004) Proton Transfer at Helium Temperatures during Dioxygen Activation by Heme Monooxygenases. *J. Am. Chem. Soc. 126*, 15960−15961.
(49) Vidossich, P., Fiorin, G., Alfonso-Prieto, M., Derat, E., Shaik, S., and Rovira, C. (2010) On the Role of Water in Peroxidase Catalysis: A Theoretical Investigation of HRP Compound I Formation. *J. Phys. Chem. B 114*, 5161−5169.
(50) Alfonso-Prieto, M., Oberhofer, H., Klein, M. L., Rovira, C., and Blumberger, J. (2011) Proton transfer drives protein radical formation in Helicobacter pylori catalase but not in Penicillium vitale catalase. *J. Am. Chem. Soc. 133*, 4285−4298.
(51) Efimov, I., Badyal, S. K., Metcalfe, C. L., Macdonald, I., Gumiero, A., Raven, E. L., and Moody, P. C. (2011) Proton delivery to ferryl heme in a heme peroxidase: enzymatic use of the Grotthuss mechanism. *J. Am. Chem. Soc. 133*, 15376−15383.
(52) Stone, K. L., Hoffart, L. M., Behan, R. K., Krebs, C., and Green, M. T. (2006) Evidence for Two Ferryl Species in Chloroperoxidase Compound II. *J. Am. Chem. Soc. 128*, 6147−6153.
(53) Schlichting, I., Berendzen, J., Chu, K., Stock, A. M., Maves, S. A., Benson, D. E., Sweet, B. M., Ringe, D., Petsko, G. A., and Sligar, S. G. (2000) The catalytic pathway of cytochrome P450cam at atomic resolution. *Science 287*, 1615−1622.
(54) Hersleth, H.-P., Uchida, T., Rohr, A. K., Teschner, T., Schuenemann, V., Kitagawa, T., Trautwein, A. X., Goerbitz, C. H., and Andersson, K. K. (2007) Crystallographic and Spectroscopic Studies of Peroxide-derived Myoglobin Compound II and Occurrence of Protonated FeIV-O. *J. Biol. Chem. 282*, 23372−23386.
(55) Leibl, W., Nitschke, W., and Hüttermann, J. (1986) Spin-density distribution in the $FeO_2]^-$ complex. Electron spin resonance of myoglobin single crystals. *Biochim. Biophys. Acta 870*, 20−30.
(56) Svistunenko, D. A. (2005) Reaction of haem containing proteins and enzymes with hydroperoxides: the radical view. *Biochim. Biophys. Acta 1707*, 127−155.
(57) Watanabe, Y., Nakajima, H., and Ueno, T. (2007) Reactivities of oxo and peroxo intermediates studied by hemoprotein mutants. *Acc. Chem. Res. 40*, 554−562.
(58) Derat, E., Kumar, D., Hirao, H., and Shaik, S. (2006) Gauging the relative oxidative powers of compound I, ferric-hydroperoxide, and the ferric-hydrogen peroxide species of cytochrome P450 toward C-H hydroxylation of a radical clock substrate. *J. Am. Chem. Soc. 128*, 473−484.